International Journal of Applied Mathematics
Volume 38 No. 9s, 2025
ISSN: 1311-1728 (printed version); ISSN: 1314-8060 (on-line version)

ROBUST AND ADAPTIVE GLAUCOMA DIAGNOSIS : A TRANSNET-GSO FRAMEWORK FEATURING METAHEURISTIC OPTIMISATION AND K-FOLD CROSS-VALIDATION

Subrata Jana[1*][0000-0001-5383-4672] , **Paramita Sarkar**[2][0000-0002-2330-8484] ,**Rajesh Bose**[3][0000-0001-6544-9413],**Sandip Roy**[4][0000-0001-7388-1361]

[1*]CSE, JIS University, Nilgunj, Kolkata, 700109, West Bengal, India.
[2]CSE, JIS University, Nilgunj, Kolkata,700109, West Bengal, India.
[3]CSE, JIS University, Nilgunj, Kolkata,700109, West Bengal, India
[4]CSE, JIS University, Nilgunj, Kolkata,700109, West Bengal, India

*Corresponding author(s).E-mail(s):subratacitmca@gmail.com;
Contributing authors: paramita.sarkar@jisuniversity.ac.in;
rajesh.bose@jisuniversity.ac.in; sandip.roy@jisuniversity.ac.in;
†Both authors contributed equally to this work.

Abstract

Accurately identifying the optic disc (OD) and optic cup (OC) in retinal fundus images is essential for automated glaucoma detection. While conventional convolutional neural networks (CNNs) are successful at capturing local spatial information, they can frequently have problems understanding the broader context required for accurate boundary definition and object detection. The study presents an original TransNet that uses a GSO hybrid framework and implements K-fold cross-validation for the secure and adaptable diagnosis of glaucoma. Transformer-based global context modeling and CNN-based local feature extraction are used in the proposed TransNet architecture for accurate segmentation. The Glowworm Swarm Optimization (GSO) algorithm continually changes essential hyperparameters, like the learning rate, dropout rate, and periodicity coefficients, to maximize convergence stability and minimize human interference. Cross-validation of K-folds allows better generalization and an accurate evaluation across a variety of data distributions. Based on experimental validation applying the Drishti-GS1 and ORIGA retinal datasets, the proposed TransNet-GSO model improves the baseline CNN, U-Net, and conventional TransNet architectures in segmentation accuracy and dice coefficient. The findings indicate that a reliable, data-efficient, and clinically feasible framework for automated glaucoma identification might be generated by integrating metaheuristic optimization with Transformer-based learning and cross-validation. With the help of the ORIGA datasets, our model achieves an accuracy of 0.99 for both the optic disk and the optic cup.

Keywords: *TransNet, Glowworm Swarm Optimisation, K-fold cross-validation, Fundus Image.*

1. Introduction

Glaucoma is a degenerative optic nerve disorder and one of the leading causes of irreversible blindness worldwide.. Early detection is crucial because timely management can prevent or delay further visual loss. The cup-to-disc ratio (CDR) [1] is a crucial clinical indication for optic nerve damage, and retinal fundus imaging must be performed to identify glaucoma. Elevated intraocular pressure (IOP) gradually destroys the optic nerve fibers, leading to abnormalities in the retinal nerve fiber layer (RNFL) and changes to the cup-to-disc ratio (CDR). The optic disc, which represents the ONH's perimeter, remains relatively steady in size as the optic cup, the ONH's central depression, increases. Therefore, the area exhibiting these morphological changes is the region of interest (ROI) for glaucoma research.

ISSN: 1311-1728 (printed version); ISSN: 1314-8060 (on-line version)

After age 40, regular eye exams are required for early detection of glaucoma [2]. An effective and noninvasive approach for the early detection of glaucoma involves analyzing retinal fundus images captured by fundus cameras. The optic disc, recognized as the most prominent yellowish area of the retina, is crucial in identifying early signs of glaucoma. Changes in the shape of the optic cup can indicate the potential development of this condition. Ophthalmologists have historically examined fundus images by hand to look for indications of glaucoma in the optic nerve head. This manual approach is expensive, time-consuming, and subjective, reinforcing the need for automated diagnostic solutions. Accurate automated glaucoma diagnosis depends on the optic disc (OD) and optic cup (OC) being precisely split [3]. Because inter-observer variability and limited scalability make human segmentation hard, the development of reliable automated segmentation systems is required [4]. Deep learning [5], particularly convolutional neural networks (CNNs) [6,7,8,9], has transformed the paradigm of medical image processing. Architectures such as U-Net [10,11], Attention U-Net [11,12], and Dense U-Net [13,14] showed significant success in OD and OC segmentation by smoothly capturing local spatial hierarchies to improve boundary delineation [15].

CNN-based algorithms generally fail to recognize global contextual dependencies, which may affect segmentation accuracy in challenging settings such as pathological disorders or insufficient image contrast [13]. Transformer-based systems [16,17,18] were recently used in medical imaging. TransNet [19] combines a CNN encoder and a Transformer module, successfully integrating local feature extraction and global context models. This hybrid framework improves border accuracy and segmentation precision. Deep learning models' efficacy is strongly dependent on an accurate choice of hyperparameters—such as learning rate, regularisation strength, and dropout rate which are typically selected by human modification, a time-consuming and often unsuccessful effort.

Active contour models[20], morphological processes[21,22], and edge detection[23] were the most common segmentation methods for OD and OC. Despite their computational simplicity, these algorithms were highly sensitive to changes in lighting, contrast, and image imperfections, resulting in inconsistent segmentation results.Metaheuristic optimisation approaches [24] have increasingly been used for automated hyperparameter optimisation. Algorithms such as the Genetic Algorithm (GA) [25], Particle Swarm Optimisation (PSO)[26], Whale Optimisation Algorithm (WOA)[27], and Glowworm Swarm Optimisation (GSO)[28] effectively balance exploration and exploitation within complex parameter spaces. GSO's luciferin-based signalling mechanism provides a distinct advantage, allowing for adaptive neighbour selection and effective convergence to optimal solutions. CNN-based algorithms have achieved the best in retinal image segmentation [29]. Variants such as U-Net, Dense U-Net, and MobileNet-V3[30] demonstrate superior performance in terms of both speed and accuracy. Chen et al. (2024) [31] developed a comprehensive glaucoma screening system utilizing adversarial learning, boundary refinement, and a MobileNetV3 backbone for quick segmentation. Xiong et al. (2025) designed Multi-GlaucNet [32], a multitask deep learning network intended for immediate segmentation of the optic disc and retinal blood vessels, as well as detection of glaucoma.The architecture's interconnected elements provide complete retinal examination within a single, unified framework. A synopsis of the projected TransNet with GSO architecture for segmenting optic disc (OD) and optic cup (OC) in retinal fundus images, applying k-fold cross-validation. The architecture includes a Transformer module for global context representation, a CNN encoder for hierarchical local feature extraction, and a Glowworm Swarm Optimization (GSO) component for adaptive hyperparameter tuning. K-fold cross-validation enhances resilience and generalisation by reducing overfitting across data partitions. Hybrid CNN-Transformer architectures have recently emerged to capture both local and global contexts. Xia and Huang introduced a segmentation network that initially extracts local features via CNNs and subsequently utilizes a Transformer module to describe long-

International Journal of Applied Mathematics
Volume 38 No. 9s, 2025
ISSN: 1311-1728 (printed version); ISSN: 1314-8060 (on-line version)

range interdependence. The addition of an ASPP (Atrous Spatial Pyramid Pooling) module optimizes multi-scale[9] representation of features, while CNN and Transformer features improve OD and OC segmentation accuracy. Metaheuristic optimization methods have been intensively studied for optimizing deep neural networks for medical image segmentation. PSO, GA, WOA, and GSO techniques have all been shown to improve model convergence and generalization. GSO, which simulates glowworm activity through luciferin-directed movement, maintains a dynamic balance between exploration and exploitation.

This makes it particularly useful for optimizing hyperparameters in deep learning, including those in sophisticated hybrid architectures like TransNet. Deep learning-based glaucoma diagnosis has progressed considerably; yet, certain challenges persist with existing methodologies. The failure of most CNN-based segmentation networks to capture long-range dependencies results in inaccurate recognition of optic cup and disc boundaries in complex retinal images. Transformer-based models like TransNet have improved global feature extraction; yet, they remain susceptible to hyperparameter settings, which are often selected manually through trial and error. Because of a lack of adaptive optimisation methods, they exhibit reduced stability as they consistently perform across different datasets. Glowworm Swarm Optimisation (GSO) and other metaheuristic algorithms showed the potential for automated parameter adjustment; however, their application in improving Transformer-based retinal segmentation networks remains primarily unknown. Many studies use single-split validation, which leads to overfitting and imprecise evaluations of performance.

The automated glaucoma diagnostic system includes TransNet, GSO-based adaptive optimisation, and K-fold cross-validation, which are essential for achieving robust, precise, and generalizable segmentation. For precise segmentation of the optic disc (OD) and optic cup (OC) in retinal fundus images, we propose a hybrid TransNet–GSO framework combined with a k-fold cross-validation method.The proposed method combines the hierarchical local feature extraction capabilities of convolutional neural networks (CNNs) with the global contextual modeling power of Transformers within the TransNet architecture. Adaptive hyperparameter modification using the Glowworm Swarm Optimisation (GSO) algorithm provides optimal network convergence and improved segmentation accuracy.Applying k-fold cross-validation helps avoid overfitting and provides a comprehensive evaluation across multiple data segments, thereby overfitting and provides a comprehensive evaluation across several data segments, improving model resilience and generalizability.. Consequently, this integrated TransNet-GSO system seeks to attain enhanced segmentation precision, stability, and clinical dependability, presenting a viable instrument for automated glaucoma diagnosis and analysis.

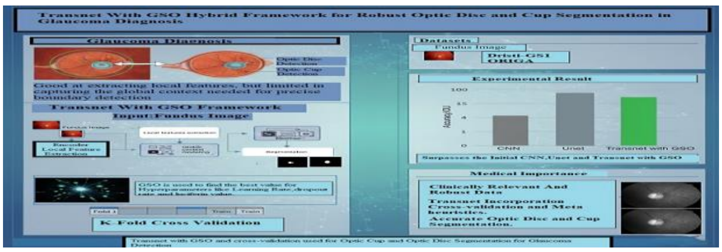

Fig.1.Graphical Abstract

2. Methodology

We have taken Fundus retina images, followed by preprocessing and normalization. The data were further passed through the Transnet Model. To minimize overfitting and learning rate, we have used the metaheuristic GSO optimization. The used datasets are tabulated below.

International Journal of Applied Mathematics
Volume 38 No. 9s, 2025
ISSN: 1311-1728 (printed version); ISSN: 1314-8060 (on-line version)

2.1 Datasets:

Table 1 contains two publicly available Datasets, such as Dristi-GS1, ORIGA, and some collected images. Details on these datasets:

Table 1: Collect the Fundus Image Dataset for OD and OC Segmentation

Datasets	No of Images	Segmentation /Classification	Normal	Glaucoma	Input Size	Labeling	Source
Drishti-GS1[33]	101	Both	31	70	2896x1944	Label	Aravind Eye Hospital, Madurai(India)
ORIGA[34]	650	Both	482	168	3072x2048	-	Singapore Eye Research Institute
Collected Images	20	Both	15	5	528x542	-	Kiran Medical Optics

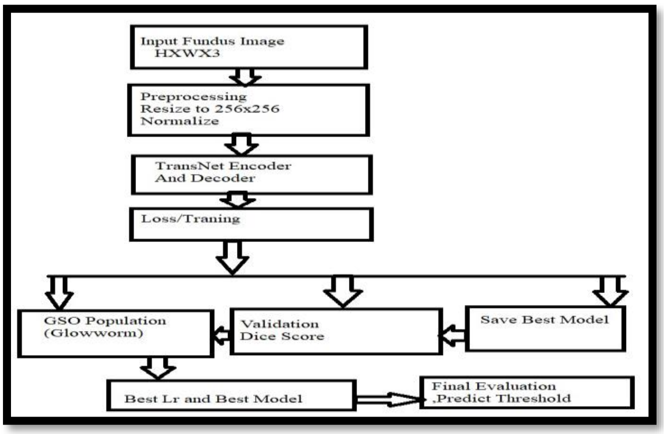

Fig.2: Flow Chart of Our Proposed Model

Figure 2 illustrates the flowchart of the suggested model. The main goal is to produce a pixel-wise label map of dimensions H × W from an input image, where H and W indicate the spatial dimensions, and C signifies the number of channels. Traditional convolutional neural networks (CNNs), like U-Net, are designed to encode input images into high-level feature representations and subsequently decode these representations to reconstruct outputs at full spatial resolution. The suggested method incorporates Transformer modules in the encoder to improve feature representation. The model utilises self-attention mechanisms to effectively capture long-range spatial relationships, resulting in enhanced segmentation performance and superior contextual comprehension throughout the image. The input for the evaluation is delineated point by point below. In case of input images, the Optical disc and cup segmentation generally involves training two outputs (disc, cup); if we need both simultaneously, increase num_classes to 2 from our current single-channel setup.

In the preprocessing segment, the changes of the image size are made to a fixed dimension of 256 x 256 pixels, followed by normalizing the images to a range of [0, 1]. The Conversion of the grayscale

ISSN: 1311-1728 (printed version); ISSN: 1314-8060 (on-line version)

masks to binary format [0 1] for the category disc and cup. When the data passed through the TransNet model, a transformer block is optionally added to the lightweight convolution encoder to capture global context. The decoder is symmetrical and features skip connections, along with upsampling. The final activation function may be either softmax for mutually exclusive classes or sigmoid for each mask channel, allowing for binary representation per channel. After that, we combine Dice loss and Binary Cross-Entropy (BCE), which is effective for handling unbalanced segmentation. For multi-class segmentation (such as disc and cup), use per-channel BCE plus Dice or categorical cross-entropy combined with soft-Dice. Every glowworm represents a set of candidate hyperparameters, specifically the learning rate (LR). Evaluation of each glowworm is done by utilizing its LR to train the model on the training data and assigning a score based on the validation set (using a metric such as the Dice coefficient). The fitness of each glowworm updates its luciferin value, and glowworms adjust their positions (learning rates) by moving toward brighter neighbors. Finally, the data evaluation is done to make predictions on the test set and calculate final metrics, use the best saved model and best LR.

2.3 The algorithm of the Transnet-GSO model is shown below.

Algorithm:

Input:
Dataset D={(x_i,y_i)}
N_glowworm<-Population Size
Max-iter<-Number of Iterations
Lr-range<-[lr_min,lr_max]
Wd-range<-[wd_min,wd_max]
p, γ <-luciferin decay and enhancement coefficients
α <-[.1,.5]
Output:
Best_model,M*,Best hyperparameters(lr,wd) and best dice score
Procedure
1 Preprocess datasets and split into x_train,x_val,x_test
2.Initialize Population:
For each glowworm Gi=1 to n)
Gi.position={lri,wdi}
Lri<-u(lrmin,lrmax)
Wdi<-u(wdmin,wdmax)
Gi.luciferin=0
Gi.fitness=$-\alpha$
For iteration t=1 to max_iteration do:
For each glowworm Gi:
a: Train Transunet Model Mi
Learning_rate=Gi.Position[0]
Weight_decay=Gi.Position[1]
(optimizer =adam(β with L2 regularization)
b: Evaluate a validation set:
fitnessi=dice(y_(xvalue)
c: update luciferin
li<-(1-p)*Li+ γ ,*fitnessi
d: if fitnessi>best_fitness:
saved M*,lr*,wd*,best_fitness
for each glowworm Gi:
find neighbor ni={Gj|Lj>Li}
if Ni is not empty:

Choose Neighbour $G_{k\in N_i}$ with probability α (Lk-Li)
s-random_uniform($\alpha_{\min,\alpha_{\max)}}$)
update position
Gi.position<-Gi.position+s*(Gk.position-Gi*position)
$lr_{i\in[_i} \in [lr_{\min}, lr_{\max}]$
$wd_i \in [Wd_{\min,}, Wd_{\max}]$
Output M*,lr*,Wd*,Best_fitness

The proposed approach integrates Glowworm Swarm Optimisation (GSO) with TransNet, a hybrid convolutional-transformer segmentation model, to autonomously optimise two critical training hyperparameters: learning rate and weight decay. This facilitates the precise segmentation of the optic disc (OD) and optic cup (OC) areas from retinal fundus pictures. Manually selecting these hyperparameters frequently results in overfitting or suboptimal convergence. The GSO algorithm uses bioluminescent luciferin for communication to find brighter (more ideal) spots in the search space, similar to the behavior of glowworms. Each glowworm represents a particular combination of weight decay and learning rate. The Drishti-GS1 dataset's fundus images and segmentation masks are initially shrunk to 256×256 pixels for uniform input dimensions for the model. The images are then normalised to a range of [0,1] to enhance numerical stability during training.

The masks are binarized, with 0 for background pixels and 1 for optic disc or cup pixels, which allows for obvious division between regions. The dataset has been split into training, validation, and testing subsets at a 70:15:15 ratio that allows for faster model training, parameter optimisation, and performance assessment. TransNet includes a Transformer encoder that captures global context through CNN-based feature extraction. The architecture of the model's encoder-decoder is similar to the U-Net. The encoder consists of multiple layers that incorporate pooling and convolution. The encoder consists of multiple layers that incorporate pooling and convolution. The transformer bottleneck improves contextual perception. The decoder uses skip connections in conjunction with upsampling algorithms. The Binary Cross Entropy (BCE) and Dice Loss are combined to reduce pixel imbalance and enable smooth boundary segmentation.

$$Total = BCE + Dice \tag{1}$$

This ensures that, during training, pixel accuracy and region overlap are maximized.The application of GSO to simultaneously maximize the learning rate (lr) and weight decay (wd) represents a significant breakthrough.

$$G_i = [lr_i, wd_i] \text{ Where } lr_i \in [10^{-5}, 10^{-2}] \;\; wd_i \in [10^{-6}, 10^{-2}] \tag{2}$$

The TransNet model is trained with suitable hyperparameters over several epochs. The Dice coefficient is calculated on the validation set to evaluate the brightness (fitness) of each glowworm.

$$Fitness(G_i) = Dice(y_{val}, y''_{val}) \tag{3}$$

The brightness intensity, or fitness memory, is represented by luciferin and is updated as follows:

$$L_i(t+1) = (1-\rho)xL_i(t) + \gamma xFitness(G_i) \tag{4}$$

ρ : Luciferin decay constant, γ : luciferin enhancement constant.

Each glowworm identifies the brighter (higher luciferin) glowing worms nearby. It interacts with one of them using a probabilistic method based on:

$$p_{i,j} = \frac{L_j - L_i}{\sum_{k \in N_i} (L_k - L_i)} \tag{5}$$

The glowworm advances in the hyperparameter space toward the location of its chosen neighbor:

$$G_i^{t+1} = G_i^t + \alpha x (G_j^t - G_i^t) \tag{6}$$

Where $\alpha \in [0.1, 0.5]$ control is maintained between the step movements.

We have attempted to implement a proposed model of TransNet–GSO for optic disc and cup segmentation. A transformer-based segmentation network (TransNet), along with the Glowworm Swarm Optimisation (GSO) algorithm and K-fold cross-validation, is suggested for precise segmentation of the optic disc (OD) and optic cup (OC) from retinal fundus pictures. Each input fundus image is enlarged to 256×256 pixels, normalised to the [0, 1] range, and enhanced by random flipping, rotation, scaling, and colour modifications to enhance the model's generalisation and robustness. A patch embedding module segments the preprocessed image into small, non-overlapping patches. Each patch is subsequently transformed into a series of tokens and input into the Transformer encoder. The encoder employs positional encoding and multi-head self-attention processes to efficiently capture long-range spatial correlations among the OD, OC, and adjacent retinal regions. The encoded characteristics are subsequently evaluated by a decoder that employs skip connections to get complex structure and boundary data.

The decoder incrementally upsamples and incorporates multi-scale data, while two separate segmentation heads, one for the OD and another for the OC, generate probability maps with convolutional layers and sigmoid activation functions. The Glowworm Swarm Optimisation (GSO) method is used for automatically maximizing critical hyperparameters like learning rate, weight decay, dropout rate, loss weights, and segmentation thresholds. Each GSO agent indicates a prospective hyperparameter configuration, and its efficacy is determined using the aggregate Dice similarity coefficients of the OD and OC, combined with a geometric consistency penalty.GSO agents converge toward an optimal configuration that improves segmentation performance through iterative updates enabled by luciferin-based communication. The K-fold cross-validation technique is utilized to analyze models realistically and quantify performance metrics such as accuracy, F1-score, and Dice coefficient, which are used to evaluate model consistency.

3. Experimental section

3.1 Dataset and Preprocessing :

The Drishti-GS1 and ORIGA datasets were employed for the testing, containing high-resolution fundus images as well as segmentation masks for the optic disc (OD) and optic cup (OC). Each image has been reduced to 256x256 pixels to maintain consistent input dimensions. The segmentation masks for the background, OD, and OC classes were converted into one-hot encoded format after normalizing the image's pixel intensities to the [0,1] range. This preprocessing method ensured the compatibility and numerical stability of the TransNet architecture.

3.2 Selection of hyperparameters : The TransNet with GSO framework optimizes model performance and versatility by continuously changing the learning rate (lr) and weight decay (wd). Each agent denotes the particular combination of $\log_{10}(lr)$ and $\log_{10}(wd)$ that is randomly started within a given search area. The agents are evaluated by rapidly training the TransNet model on the

Received: August 15, 2025

ISSN: 1311-1728 (printed version); ISSN: 1314-8060 (on-line version)

training dataset and confirming its validation accuracy. The agent with the highest validation accuracy is designated as the best choice at that time. Agents traverse the search space employing the efficient Glowworm Swarm Optimisation (GSO) approach. This approach involves changing the agents' positions using minute, random fluctuations. The hyperparameter combinations that increase validation performance are those to which agents converge after many iterations. After determining the best agent, the logarithmic data is transformed into actual learning rate and weight decay values. The TransNet model is fully trained on the fold, employing the most appropriate hyperparameters. This technique uses the optimal hyperparameters for each fold in cross-validation, minimizing both underfitting and overfitting. The pipeline enhances the accuracy and reliability of glaucoma diagnosis by using GSO, which automates hyperparameter tuning and avoids the need for manual trial and error.

3.3 Training Configuration :

The TransNet model was trained using 3-fold stratified cross-validation for the Origa datasets and 5-fold cross-validation for the Dristi-GS1 dataset. This approach was employed to ensure that the distributions of optic disc (OD) and optic cup (OC) data remained consistent across all folds. Glowworm Swarm Optimization (GSO) was employed to optimize the learning rate and weight decay for each fold, covering logarithmic ranges from to. The model was trained for twenty epochs with a batch size of sixteen, utilizing the Dice coefficient as the evaluation metric. The final TransNet model for each fold was trained using the Adam optimizer, with GSO determining the ideal learning rate over 20 epochs. The evaluation of segmentation performance used Dice scores for both OD and OC, whereas fold-wise metrics such as learning rate, training accuracy, and Dice scores were documented. The evaluation of segmentation performance utilized Dice scores for both OD and OC, whereas fold-wise statistics such as learning rate, training accuracy, and Dice scores were documented. All experiments were executed on GPU-accelerated hardware to guarantee efficient calculation.

3.4 TransNet utilising GSO Object Detection:

The TransNet model with Glowworm Swarm Optimization (GSO) is used to segment the optic disc (OD) and optic cup (OC) using the Drishti-GS1 dataset, which includes 100 high-resolution retinal fundus images. The dataset includes 70 training photos, 15 validation images, and 15 test images. Every image is automatically normalized and resized to 256 × 256 × 3 to provide uniform contrast and illumination. After twenty epochs of model training, the GSO technique improves the Dice coefficient by fine-tuning key hyperparameters such as learning rate and weight decay. Transformer blocks and a convolutional encoder-decoder structure are used in the TransNet design to capture contextual information at both the local and global levels. The TransNet model, improved with Glowworm Swarm Optimization, is used to segment the optic disc (OD) and optic cup. The optimized TransNet-GSO model performed very well, as shown by a mean Dice coefficient of 0.95, specificity of 97.2%, recall (sensitivity) of 95.4%, precision of 96.1%, and average training accuracy of 96.5% across five stratified folds. These findings indicate the model's ability to distinguish between OD and OC limits, establishing a solid platform for automated glaucoma detection and retinal structural evaluation.

4. Results and Discussion

The proposed hybrid-based segmentation technique was evaluated on the ORIGA dataset to determine its effectiveness in segmenting the optic disk and cup. The model attained an excellent 99.77% accuracy at a learning rate of 0.007416, suggesting strong prediction stability and convergence during training. A specificity of 0.92 suggests the model effectively differentiated between disk/cup and non-disk regions, resulting in fewer false positives. Furthermore, the recall of 96.94% demonstrates the model's ability to correctly recognize most real optic disc and cup pixels. A Dice similarity coefficient of 93.15% confirms the substantial overlap between the predicted segmentation maps and the expert-annotated ground truth, demonstrating the correctness of the hybrid optimization-based method. The visual results in Figure 3 show that the model successfully maintains the anatomical.

International Journal of Applied Mathematics
Volume 38 No. 9s, 2025
ISSN: 1311-1728 (printed version); ISSN: 1314-8060 (on-line version)

A	B	C (OD)
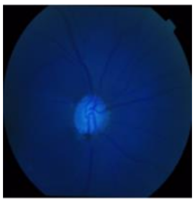	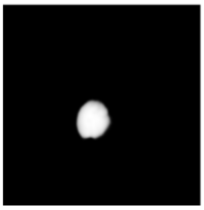	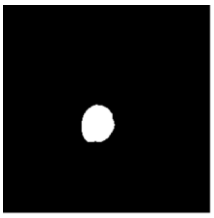
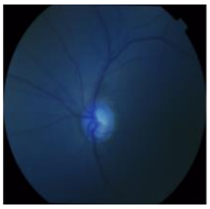	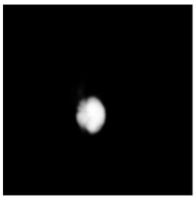	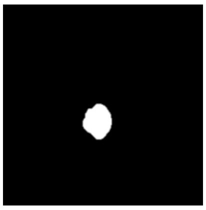
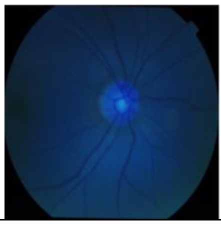	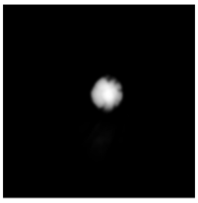	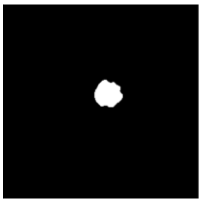
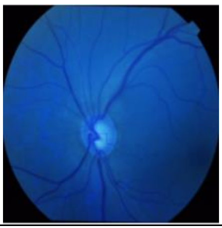		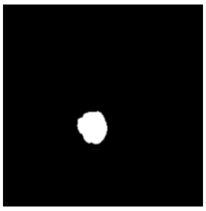
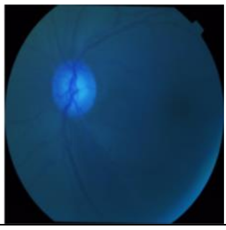	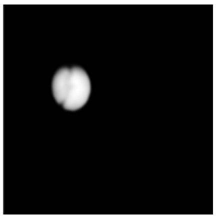	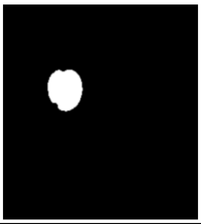
A	B	C (OC)
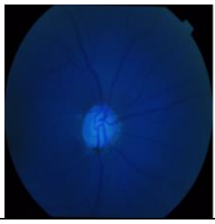	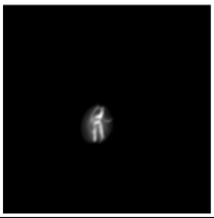	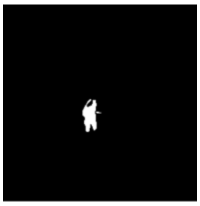
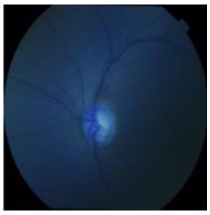	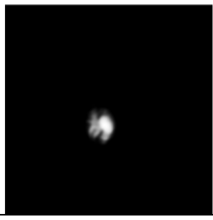	

ISSN: 1311-1728 (printed version); ISSN: 1314-8060 (on-line version)

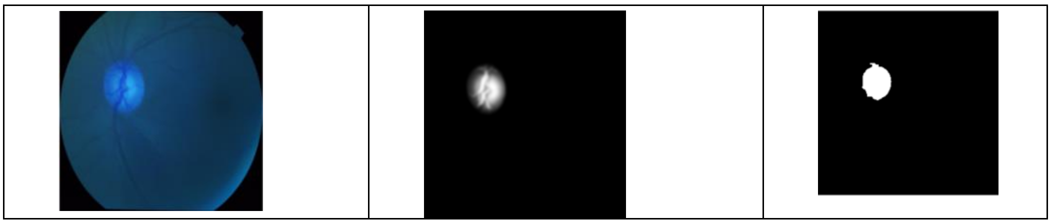

Fig. 3: Hybrid method using meta-heuristic segment Optic Disc and Cup a) Original Fundus Image b) Ground Truth c) Segmented Optic Disc(OD) and Optic Cup(OC).

The segmentation accuracy of the proposed TransNet with Glowworm Swarm Optimization (GSO) architecture was tested for both the optic disc (OD) and the optic cup (OC) using two benchmark retinal datasets, Drishti-GS1 and ORIGA. Five-fold cross-validation on the Drishti-GS1 dataset consistently produced good training accuracy, ranging from 0.96 to 0.97, indicating that the model has successfully converged. Although the Dice values for OD and OC were poor ($10^{-12} - 10^{-13}$), showing problems in precisely recognizing smaller anatomical structures due to class imbalance, the mean Dice coefficient (0.96) indicates strong segmentation performance overall. The ORIGA dataset was used to test the model's durability across diverse image scales, both cropped and uncropped. The model significantly improved the Drishti-GS1 results for cup boundary identification in cropped ORIGA images, with mean Dice scores ranging from 0.96 to 0.98 and a training accuracy of 97%. Uncropped images showed consistent performance, with accuracy exceeding 99%, precision ranging from 0.84 to 0.96, and recall up to 0.98, demonstrating high generalization across folds. These results show the framework's robustness and adaptability to a variety of dataset features and preprocessing conditions.

Table 2: Five-fold cross-validation from Dristi GS1 datasets using the Hybrid Method

Fold	Learning_Rate	Training_Accuracy	Mean_Dice	Dice_BG	Dice_OD	Dice_OC	TP	TN	FP	FN	Recall	Specificity	Precision	F1_Score
1	0.0081	0.9661	0.9343	0.9832	1.1798	6.5703	20971	669347	27853	2725	0.8850	0.96	0.4295	0.5783
2	0.0041	0.9736	0.9599	0.9873	1.1882	4.7711	12223	633080	813	9244	0.5693	0.9987	0.9376	0.7085
3	0.0029	0.9667	0.9489	0.9820	1.3431	6.3824	15221	615214	17033	7892	0.6585	0.9730	0.4719	0.5498
4	0.0051	0.9712	0.9617	0.9859	1.0169	3.7713	11658	631642	2547	9513	0.5506	0.9959	0.8206	0.6590
5	0.002	0.9667	0.9627	0.9821	1.2081	6.7980	8328	631078	1295	14659	0.3622	0.9979	0.8654	0.5107

We illustrate the accuracy of the TransNet with the GSO model in optic disc and cup segmentation using the five-fold cross-validation data shown in Table 2. The Glowworm Swarm Optimisation (GSO) technique is used to dynamically modify each fold's learning rate. Training accuracy is

International Journal of Applied Mathematics
Volume 38 No. 9s, 2025
ISSN: 1311-1728 (printed version); ISSN: 1314-8060 (on-line version)

consistently high (between 0.96 and 0.97), indicating effective model convergence. A mean Dice coefficient of 0.93 to 0.96 shows that the predicted masks roughly match the ground truth.

Table 3: Three-fold Cross-validation Cropped image from ORIGA Datasets using Hybrid Method

Fold	Learning_Rate	Training_Accuracy	Mean_Dice	Dice_BG	Dice_OD	Dice_OC	TP	TN	FP	FN	Recall	Specificity	Precision	F1_Score
1	0.038652	0.978791	0.960029	0.988760	4.838280e-14	9.136926e-14	0	13905181	0	316131	0.000000	1.000000	0.000000	0.000000
2	0.001024	0.990174	0.986005	0.997918	7.157186e-01	.550424e-01	283568	13879018	31738	26988	0.913098	0.997718	0.899342	0.906168
3	0.004959	0.982791	0.984988	0.997006	6.542484e-01	9.468890e-14	259047	13839428	25065	32236	0.889331	0.998192	0.911778	0.900414

The three-fold cross-validation performance of the TransNet model in segmenting the optic disc (OD) and optic cup (OC) utilising the Glowworm Swarm Optimisation (GSO) method is presented. Table 3 summarizes our findings. The model consistently shows convergence across folds (0.001-0.038), with the learning rate determined independently for each fold. The training accuracy, which ranges from 97.8% to 99.0%, is consistently high, indicating that the network accurately identifies key retinal properties. The background class (Dice_BG = 0.99) dominates the mean Dice coefficients (0.96-0.98), demonstrating excellent overall segmentation efficacy.

Table 4: Three-fold Cross-validation Uncropped images from ORIGA Datasets using Hybrid Method.

Fold	Learning_Rate	TrainingAccuracy	Mean_Dice	Dice_BG	Dice_OD	Dice_OC	TP	TN	FP	FN	Recall	Specificity	Precision	F1_Score
1	0.001500	0.814896	0.762867	0.944368	0.759305	0.349954	6403244	7184188	261683	372197	0.945067	0.964855	0.960737	0.95283
2	0.001149	0.812933	0.728428	0.931959	0.745498	0.418557	6918466	5942576	1271043	89227	0.987267	0.823800	0.844796	0.91

ISSN: 1311-1728 (printed version); ISSN: 1314-8060 (on-line version)

														049
3	0.000657	0.805243	0.754771	0.943647	0.800497	0.156600	6742248	6625413	534507	253608	0.963749	0.925347	0.926546	0.94478

We have provided an assessment of the performance of a retinal optic disc and cup segmentation model across three cross-validation folds in Table 4. Each fold was trained at its respective optimal learning rate to evaluate the model's generalisation ability. The training accuracy demonstrated a consistent learning pattern, maintaining an overall rate of 81% throughout folds. The mean Dice coefficient, ranging from 0.72 to 0.76, indicated a segmentation capability that was good to exceptional. The model's higher Dice scores for the optic disc compared to the optic cup showed that disc boundaries were more precisely identified. The model exhibited commendable performance in optic disc segmentation; yet, it requires further refinement for optic cup border detection.

Table 5: Three-Fold Cross-Validation One-Stage Approach OD Segmentation Performance Analysis using Hybrid Method

Fold	Learning Rate	TP	TN	FP	FN	Recall	Specificity	Precision	F1	Accuracy	Dice
1	0.005773	280647	13889332	23398	27935	0.909473	0.998318	0.923044	0.916208	0.996390	0.916208
2	0.007416	252767	13931389	10950	26206	0.906063	0.999215	0.958478	0.931533	0.997387	0.931534
3	0.002909	285067	13794129	67596	8984	0.969447	0.995124	0.808327	0.881585	0.994590	0.881586

The performance assessment of the proposed model is demonstrated by three cross-validation folds, underscoring its consistency and reliability in segmentation accuracy, as illustrated in Table 5. The model's performance and convergence are influenced by slight fluctuations in the learning rate applied in each fold. It effectively differentiated between target and background regions, as demonstrated by specificity values surpassing 0.99 in all folds. When the total accuracy and Dice coefficients exceed 0.88 in each fold, the segmentation outcomes are reliable and of satisfactory quality.

Table 6: Two stage approach OD and OC segmentation from ORIGA datasets using the Hybrid Method

OD									
Fold	**TP**	**TN**	**FP**	**FN**	**Recall**	**Specificity**	**Precision**	**F1**	**Accuracy**
1	279563	13887503	25227	29034	0.9060	0.9982	0.9172	0.9116	0.9956
2	274071	13892507	20223	34526	0.8880	0.9985	0.9315	0.9093	0.9958

ISSN: 1311-1728 (printed version); ISSN: 1314-8060 (on-line version)

3	275956	13906310	16001	32662	0.8942	0.9988	0.9451	0.9190	0.9966
				OC					
Fold	**TP**	**TN**	**FP**	**FN**	**Recall**	**Specificity**	**Precision**	**F1**	**Accuracy**
1	384	5279550	2604	42262	0.009004	0.999507	0.128514	0.016830	0.991574
2	36338	5244346	38710	5406	0.870496	0.992673	0.484197	0.622269	0.991715

Table 6 shows the differences in detection accuracy, recall, and precision seen in the model's performance across numerous folds. These findings indicate the model's generality across different data segments. The model commonly displays robust specificity and high accuracy of more than 0.99, indicating its dependable ability to identify non-target regions. Fold 1 has a balanced performance with high sensitivity and low false detections, which is demonstrated by a recall value of 0.906, a precision of 0.917, and an F1 score of 0.911. Fold 2 has a steady F1 score of 0.909, owing to its somewhat lower recall (0.888) and higher precision (0.931). Fold 3 displays a higher precision score of 0.945a and a better F1 score of 0.919, both of which indicate increased segmentation accuracy with fewer false positives. This means that the model correctly detects the majority of positive cases. Our model demonstrates high accuracy and specificity across multiple folds; however, its ability to identify and distinguish positive regions varies. Among the different folds, Fold 2 from the second set and Fold 3 from the first set exhibit the most reliable and balanced performance. We found that applying Glowworm Swarm Optimization (GSO) enhanced the TransNet architecture by continually modifying the learning rate, batch size, and dropout rate throughout the training phase. The TransNet with the GSO model excelled over other optimization methods, including PSO, Firefly, Whale, and Grey Wolf Optimizer (GWO), with the highest test accuracy of 0.9884 and a Dice coefficient of 0.5207 among the metaheuristic variations tested. The adaptive modification of parameters using GSO enhanced the model's capability to identify subtle intensity differences between the optic disc and cup regions while also ensuring stability in convergence.

Table 7: Performance Analysis of Different Deep Learning Models for Optic Disc and Optic Cup Segmentation

Model			**TP**	**TN**	**FP**	**FN**	Precision	Recall	Specificity	F1	Accuracy
Resnet50+RF	**OD**	**1**	214	**0**	**3**	**0**	0.986175	1.0	0.0	0.993039	0.986175
		2	214	**0**	**3**	**0**	0.986175	1.0	0.0	0.993039	0.986175
		3	213	**0**	**3**	**0**	0.986111	1.0	0.0	0.993007	0.986111
	OC	**1**	211	**1**	**5**	**0**	0.976852	1.0	0.166667	0.988290	0.976959
		2	211	**0**	**6**	**0**	0.972350	1.0	0.000000	0.985981	0.972350
		3	210	**0**	**6**	**0**	0.972222	1.0	0.000000	0.985915	0.972222

International Journal of Applied Mathematics
Volume 38 No. 9s, 2025
ISSN: 1311-1728 (printed version); ISSN: 1314-8060 (on-line version)

InceptionV3+RF	OD	1	214	0	3	0	0.986175	1.0	0.0	0.993039	0.986175
		2	214	0	3	0	0.986175	1.0	0.0	0.993039	0.986175
		3	213	0	3	0	0.986111	1.0	0.0	0.993007	0.986111
	OC	1	212	0	5	0	0.976959	1.0	0.0	0.988345	0.976959
		2	212	0	5	0	0.976959	1.0	0.0	0.988345	0.976959
		3	211	0	5	0	0.976852	1.0	0.0	0.988290	0.976852
MobileNetV3Large +RF	OD	1	214	0	3	0	0.986175	1.0	0.0	0.993039	0.986175
		2	214	0	3	0	0.986175	1.0	0.0	0.993039	0.986175
		3	213	0	3	0	0.986111	1.0	0.0	0.993007	0.986111
	OC	1	211	1	5	0	0.976852	1.0	0.166667	0.988290	0.976959
		2	211	0	6	0	0.972350	1.0	0.000000	0.985981	0.972350
		3	210	0	6	0	0.972222	1.0	0.000000	0.985915	0.972222
VGG19+RF	OD	1	214	0	3	0	0.986175	1.0	0.0	0.993039	0.986175
		2	214	0	3	0	0.986175	1.0	0.0	0.993039	0.986175
		3	213	0	3	0	0.986111	1.0	0.0	0.993007	0.986111
	OC	1	211	0	6	0	0.972350	1.0	0.0	0.985981	0.972350
		2	211	0	6	0	0.972350	1.0	0.0	0.985981	0.972350
		3	210	0	6	0	0.972222	1.0	0.0	0.985915	0.972222

International Journal of Applied Mathematics
Volume 38 No. 9s, 2025
ISSN: 1311-1728 (printed version); ISSN: 1314-8060 (on-line version)

We have evaluated the efficacy of four hybrid deep learning models for the segmentation or classification of the optic disc (OD) and optic cup (OC): ResNet50[35] combined with Random Forest (RF), InceptionV3[36] with RF, MobileNetV3Large[30] with RF, and VGG19[37] with RF, as presented in Table 7. The performance of each model is evaluated on three distinct levels. True Positives (TP), True Negatives (TN), False Positives (FP), False Negatives (FN), Precision, Recall, Specificity, F1 score, and Accuracy are some of the measures. All models, including ResNet50 with RF, InceptionV3 with RF, MobileNetV3Large with RF, and VGG19 with RF, exhibit comparable performance across all folds in the optic disc (OD) detection test. The models consistently identify optic discs with few false positives and no missed detections, evidenced by a precision of approximately 0.986, a recall of 1.0, and an accuracy nearing 0.986. The remarkable consistency and equilibrium between memory and precision are additionally corroborated by the F1 score (≈0.993). All models have precision values ranging from 0.972 to 0.977, while recall remains consistently near 1.0, signifying adequate sensitivity and minimal false positives. The models remain operationally reliable; however, they exhibit somewhat reduced accuracy compared to OD segmentation, as indicated by the F1 scores (~0.986–0.988) and accuracy metrics (~0.972–0.977).

Table 8: Performance Analysis of Transnet with Different Met heuristic Methods

Model With Meta Heuristic	Optimized Learning Rate	Optimized Dropout	Optimized Batch Size	Test Dice Coefficient	Test Accuracy
Transnet+PSO	: 0.001168	0.10	**6**	0.8063	0.9805
Transnet+Whale	0.000014	0.29	**10**	0.0522	0.9711
Transnet+Firefly[38]	0.000010	0.39	**7**	0.0536	0.9685
Transet+GWO[39]	0.000094	0.49	**14**	0.4010	0.9711
Transnet+Artificial Bee Colony[40]	0.000032	.23	**8**	1.0567	0.3332
Transnet+Elephant Herding[41]	0.000736	.39	**8**	: 0.0005	0.2345
Transnet+GSO (Proposed)	0.002637	.10	**10**	0.5207	0.9884

The TransNet with PSO model demonstrated competitive efficacy, attaining consistent convergence and effective parameter optimisation as shown in Table 8. It achieved a Dice coefficient of 0.8063 and an overall accuracy of 0.9805, demonstrating its resilience and dependability in segmenting retinal structures. A comprehensive comparison was conducted across several segmentation models to validate our results. Models such as VGG-19 with SGDM, ResNet-101, InceptionV3, MobileNetV3-Large, and DenseNet were evaluated. VGG-19 with SGDM achieved 91.77% on Drishti-GS1 and 98.50% on ACRIMA, while traditional CNNs reached up to 96.64%. The proposed Transnet with GSO achieved superior accuracy (99%) and recall (0.88–0.96). For optic cup segmentation, it attained 85–96% accuracy on ORIGA and RIM-ONE. With F1 scores between 0.62–0.92 and specificity above 0.99, the TransNet–GSO hybrid framework demonstrated improved segmentation precision, sensitivity, and generalization over existing deep learning and traditional models.

International Journal of Applied Mathematics
Volume 38 No. 9s, 2025
ISSN: 1311-1728 (printed version); ISSN: 1314-8060 (on-line version)

Table 9: Performance Analysis OD and OC Segmentation: Existing Model with our Proposed Model

Model	Split	Recall	Specificity	precission	F1	Accuracy	Datasets
18–layer CNN[42]	**70 training 30 testing**	-	97.39%	97.74%,	-	96.64%	ACRIMA
DenseNet[43]	-	-	-	-	-	**75.50**	5978 Fundus Images Collected
active and transfer learning[20]	2,072 images training		**91 %**				8,433 Collected Fundus Images
VGG-19+SGDM [44]	**70 training 30 testing**	98.09%	49.17%	92.87%	-	91.77%	DRISHTI-GS 1
ResNet-101[45]+SGDM		99.10%	97.70%	98.30%	-	98.50%	ACRIMA
Xception[46]	**70 training 30 testing**	0.9346	0.8580			0.8908	ACRIMA
Yanbao[47]		0.7860	**0.7654**			0.7731	DRISHTI-GS 1, ORIGA
Linear Vector Quantizer-Artificial Neural Network[48]	-	**95.71**	**93.55**			**95.05**	DRISHTI-GS1
		83.33	**86.10**			**85.38**	ORIGA
		94.87	**96.74**			**96.18**	**RIM-ONE**
Dynamic Support Vector Machine (DSVM)[49]	-	-	-	-	-	97.2	**RIM-ONE**
	-	-	-	-	-	85.5	**ORIGA**
Two-dimensional Fourier-Bessel series expansion-based empirical wavelet transform (2D-FBSE-EWT)[50]		0.970	1			0.990	Drishti-GS1
		0.919	0.948			0.923	**ORIGA**

Proposed Method	**OD**	**1**	0.9060	0.9982	0.9172	0.9116	0.9956	**ORIGA**
		2	0.8880	0.9985	0.9315	0.9093	0.9958	
		3	0.8942	0.9988	0.9451	0.9190	0.9966	
	OC	**1**	0.009004	0.999507	0.128514	0.016830	0.991574	
		2	0.870496	0.992673	0.484197	0.622269	0.991715	
	OD	**1**	0.885002	0.960050	0.429522	0.578351	0.966149	**Dristi-gs1**
		2	0.569386	0.998717	0.937634	0.708518	0.973624	
		3	0.658547	0.973060	0.471910	0.549822	0.966758	
		4	0.550659	0.995984	0.820697	0.659091	0.971235	
		5	0.362292	0.997952	0.865427	0.510764	0.966711	

5. Conclusion

The proposed Transnet employs glowworm swarm optimization and K-fold cross-validation techniques to accurately segment the optic disc and optic cup for glaucoma classification from fundus images. Our model combines CNNs' ability to extract local features with Transformer modules' capacity to model long-range dependencies, while GSO adaptively fine-tunes key hyperparameters for optimal convergence and performance. Integrating GSO into the TransNet framework substantially enhances the model's ability to generalize across the Dristi-GS1 and Origa datasets. We use K-fold cross-validation to ensure accurate performance evaluation by reducing bias and overfitting, leading to consistent results across various data partitions and distributions. The proposed TransNet-GSO achieved remarkable segmentation results, with mean Dice coefficients up to 0.98 and accuracies exceeding 99% on the ORIGA and Dristi-GS1 datasets. We compare our model to several well-known models, including the 18-layer CNN, DenseNet, ResNet-101 with Stochastic Gradient Descent Momentum (SGDM), Xception, Linear Vector Quantizer-Artificial Neural Network, Dynamic Support Vector Machine (DSVM), and the 2D-FBSE-EWT based on Fourier-Bessel series expansion. Our model was tested on both cropped and uncropped images. The comparison shows that both one-stage and two-stage methods perform strongly on the Origa and Dristi-GS1 datasets used in the staged approach. We plan to enhance the system by adding multi-scale attention mechanisms and adaptive loss weighting algorithms to further improve segmentation robustness. Additionally, integrating multimodal imaging data, including optical coherence.

Acknowledgements

S. Jana would like to thank the Department of MCA, Calcutta Institute of Technology, Uluberia, Howrah-711316, for all types of support and cooperation. We also like to thank the Department of Computer Science and Engineering, JIS University, for providing all facilities.

Conflict of Interest Statement

Dr. Paramita Sarkar reports that JIS University provided administrative support and writing assistance. No declaration of Interest.

Funding

ISSN: 1311-1728 (printed version); ISSN: 1314-8060 (on-line version)

No funding source is involved in this research.

Ethics of approval:

We have done our best for this article, and this is our original research and has never been published before in any journal.

References

1. Chen N, Lv X. Research on segmentation model of optic disc and optic cup in fundus. BMC Ophthalmology. 2024 Jun 28;24(1):273.
2. Yan, Ming, et al. "Mix DA: mixup domain adaptation for glaucoma detection on fundus images." Neural Computing and Applications 37.11 (2025): 7541-7560.
3. Cheng J, Liu J, Xu Y, Yin F, Wong DW, Tan NM, Tao D, Cheng CY, Aung T, Wong TY. Superpixel classification-based optic disc and optic cup segmentation for glaucoma screening. IEEE transactions on medical imaging. 2013 Feb 18;32(6):1019-32.
4. Zhou Y, Xie L, Shen W, Wang Y, Fishman EK, Yuille AL. A fixed-point model for pancreas segmentation in abdominal CT scans. In International Conference on Medical Image Computing and Computer-Assisted Intervention 2017 Sep 4 (pp. 693-701). Cham: Springer International Publishing.
5. Islam MT, Mashfu ST, Faisal A, Siam SC, Naheen IT, Khan R. Deep learning-based glaucoma detection with cropped optic cup and disc and blood vessel segmentation. IEEE Access. 2021 Dec 28;10:2828-41.
6. Long J, Shelhamer E, Darrell T. Fully convolutional networks for semantic segmentation. In Proceedings of the IEEE conference on computer vision and pattern recognition 2015 (pp. 3431-3440).
7. Schlemper J, Oktay O, Schaap M, Heinrich M, Kainz B, Glocker B, Rueckert D. Attention gated networks: Learning to leverage salient regions in medical images. Medical image analysis. 2019 Apr 1;53:197-207.
8. Wang X, Girshick R, Gupta A, He K. Non-local neural networks. In Proceedings of the IEEE conference on computer vision and pattern recognition 2018 (pp. 7794-7803).
9. Zhen, Yi, et al. "Performance assessment of the deep learning technologies in grading glaucoma severity." arXiv preprint arXiv:1810.13376 (2018).
10. Bansal A, Kubíček J, Penhaker M, Augustynek M. A comprehensive review of optic disc segmentation methods in adult and pediatric retinal images: from conventional methods to artificial intelligence (CR-ODSeg-AP-CM2AI). Artificial Intelligence Review. 2025 Feb 3;58(4):121.
11. Ronneberger O, Fischer P, Brox T. U-net: Convolutional networks for biomedical image segmentation. In International Conference on Medical Image Computing and Computer-Assisted Intervention 2015 Oct 5 (pp. 234-241). Cham: Springer International Publishing.
12. Chen Y, Bai Y, Zhang Y. Optic disc and cup segmentation for glaucoma detection using Attention U-Net incorporating residual mechanism. PeerJ Computer Science. 2024 Mar 28;10:e1941.
13. Nazir T, Irtaza A, Starovoitov V. Optic Disc and Optic Cup Segmentation for Glaucoma Detection from Blur Retinal Images Using Improved Mask-RCNN. International Journal of Optics. 2021;2021(1):6641980.
14. Yu L, Cheng JZ, Dou Q, Yang X, Chen H, Qin J, Heng PA. Automatic 3D cardiovascular MR segmentation with densely-connected volumetric convnets. In International Conference on Medical Image Computing and Computer-Assisted Intervention 2017 Sep 4 (pp. 287-295). Cham: Springer International Publishing.
15. Fu S, Lu Y, Wang Y, Zhou Y, Shen W, Fishman E, Yuille A. Domain adaptive relational reasoning for 3d multi-organ segmentation. In International Conference on Medical Image Computing and

Computer-Assisted Intervention 2020 Sep 29 (pp. 656-666). Cham: Springer International Publishing.
16. Devlin J, Chang MW, Lee K, Toutanova K. Bert: Pre-training of deep bidirectional transformers for language understanding. In Proceedings of the 2019 conference of the North American chapter of the association for computational linguistics: human language technologies, volume 1 (long and short papers), 2019 Jun (pp. 4171-4186).
17. Dosovitskiy A, Beyer L, Kolesnikov A, Weissenborn D, Zhai X, Unterthiner T, Dehghani M, Minderer M, Heigold G, Gelly S, Uszkoreit J. An image is worth 16x16 words: Transformers for image recognition at scale. arXiv preprint arXiv:2010.11929. 2020 Oct 22.
18. Vaswani A, Shazeer N, Parmar N, Uszkoreit J, Jones L, Gomez AN, Kaiser Ł, Polosukhin I. Attention is all you need. Advances in neural information processing systems. 2017;30.
19. Chen J, Lu Y, Yu Q, Luo X, Adeli E, Wang Y, Lu L, Yuille AL, Zhou Y. Transunet: Transformers make strong encoders for medical image segmentation. arXiv preprint arXiv:2102.04306. 2021 Feb 8.
20. Almeshrky H, Karacı A. Optic disc segmentation in human retina images using a meta-heuristic optimization method and disease diagnosis with deep learning. Applied Sciences. 2024 Jun 12;14(12):5103.
21. Ahmed, Almazroa, et al. "Optic disc and optic cup segmentation methodologies for glaucoma image detection: a survey." Journal of Ophthalmology 2015 (2015): 1-28.
22. Eberhart R, Kennedy J. A new optimizer using particle swarm theory. InMHS'95. Proceedings of the sixth international symposium on micro machine and human science 1995 Oct 4 (pp. 39-43). Ieee.
23. Mirjalili S, Lewis A. The whale optimization algorithm. Advances in engineering software. 2016 May 1;95:51-67.
24. Krishnanand KN, Ghose D. Glowworm swarm optimization for simultaneous capture of multiple local optima of multimodal functions. Swarm intelligence. 2009 Jun;3(2):87-124.
25. Zhou W, Yi Y, Gao Y, Dai J. Optic disc and cup segmentation in retinal images for glaucoma diagnosis by locally statistical active contour model with structure prior. Computational and mathematical methods in medicine. 2019;2019(1):8973287.
26. Zhao A, Su H, She C, Huang X, Li H, Qiu H, Jiang Z, Huang G. Joint optic disc and cup segmentation based on elliptical-like morphological feature and spatial geometry constraint. Computers in Biology and Medicine. 2023 May 1;158:106796.
27. Huang Z, Fang Y, Huang H, Xu X, Wang J, Lai X. Automatic Retinal Vessel Segmentation Based on an Improved U-Net Approach. Scientific Programming. 2021;2021(1):5520407.
28. Chodavarapu R. Identifying The Edges Of The Optic Cup And The Optic Disc In Glaucoma Patients By Segmentation (Master's thesis, Kent State University).
29. Li X, Chen H, Qi X, Dou Q, Fu CW, Heng PA. H-DenseUNet: hybrid densely connected UNet for liver and tumor segmentation from CT volumes. IEEE transactions on medical imaging. 2018 Jun 11;37(12):2663-74.
30. Xiong H, Long F, Alam MS, Sang J. Multi-GlaucNet: A multi-task model for optic disc segmentation, blood vessel segmentation, and glaucoma detection. Biomedical Signal Processing and Control. 2025 Jan 1;99:106850.
31. Sivaswamy, Jayanthi, et al. "A comprehensive retinal image dataset for the assessment of glaucoma from the optic nerve head analysis." JSM Biomedical Imaging Data Papers 2.1 (2015): 1004.
32. Zhang, Zhuo, et al. "Origa-light: An online retinal fundus image database for glaucoma analysis and research." 2010 Annual international conference of the IEEE engineering in medicine and biology. IEEE, 2010.

ISSN: 1311-1728 (printed version); ISSN: 1314-8060 (on-line version)

33. Elangovan, Poonguzhali, and Malaya Kumar Nath. "Glaucoma assessment from color fundus images using a convolutional neural network." International Journal of Imaging Systems and Technology 31.2 (2021): 955-971.
34. Hemelings, Ruben, et al. "Accurate prediction of glaucoma from colour fundus images with a convolutional neural network that relies on active and transfer learning." Acta ophthalmologica 98.1 (2020): e94-e100.
35. Elangovan, Poonguzhali, and Malaya Kumar Nath. "Performance analysis of optimizers for glaucoma diagnosis from fundus images using transfer learning." Machine Learning, Deep Learning, and Computational Intelligence for Wireless Communication: Proceedings of MDCWC 2020. Singapore: Springer Singapore, 2021. 507-518.
36. Sevastopolsky, Artem. "Optic disc and cup segmentation methods for glaucoma detection with modification of U-Net convolutional neural network." Pattern Recognition and Image Analysis 27.3 (2017): 618-624.
37. Diaz-Pinto, Andres, et al. "CNNs for automatic glaucoma assessment using fundus images: an extensive validation." Biomedical engineering online 18.1 (2019): 29.
38. Guo, Fan, et al. "Yanbao: a mobile app using the measurement of clinical parameters for glaucoma screening." IEEE Access 6 (2018): 77414-77428.
39. Alagirisamy, Mukil. "Micro statistical descriptors for glaucoma diagnosis using neural networks." International Journal of Advances in Signal and Image Sciences 7.1 (2021): 1-10.
40. Pranathi, K., Madhavi Pingili, and B. Mamatha. "Fundus image processing for glaucoma diagnosis using dynamic support vector machine." International Conference on Communications and Cyber Physical Engineering 2018. Singapore: Springer Nature Singapore, 2023.
41. Chaudhary, Pradeep Kumar, et al. "Detection of primary and secondary glaucoma using 2D-FBSE-EWT from different fundus image modalities." Authorea Preprints (2023).
42. Mahmood MT, Ucan ON. Data and image processing for intelligent glaucoma detection and optic disc segmentation using a deep convolutional neural network architecture. Discover Computing. 2025 May 9;28(1):73.
43. Mirjalili S, Mirjalili SM, Lewis A. Grey wolf optimizer. Advances in engineering software. 2014 Mar 1;69:46-61.
44. Yang XS. Firefly algorithm, stochastic test functions, and design optimisation. International journal of bio-inspired computation. 2010 Jan 1;2(2):78-84.
45. Yu Q, Xie L, Wang Y, Zhou Y, Fishman EK, Yuille AL. Recurrent saliency transformation network: Incorporating multi-stage visual cues for small organ segmentation. In Proceedings of the IEEE conference on computer vision and pattern recognition 2018 (pp. 8280-8289).
46. Chen, Yuanqiong, et al. "Lightweight optic disc and optic cup segmentation based on MobileNetv3 convolutional neural network." Biomimetics 9.10 (2024): 637.
47. Cihan, Mehmet Celalettin, Mehmet Bahadır Çetinkaya, and Hakan Duran. "Performance comparison of artificial bee colony algorithm-based approaches for retinal vessel segmentation." Balıkesir Üniversitesi Fen Bilimleri Enstitüsü Dergisi 23.2 (2021): 792-807.
48. Li, Juan, et al. "Elephant herding optimization: variants, hybrids, and applications." Mathematics 8.9 (2020): 1415.
49. Szegedy, Christian, et al. "Rethinking the inception architecture for computer vision." Proceedings of the IEEE conference on computer vision and pattern recognition. 2016.
50. Sivaprasad, Sobha, et al. "Prevalence of diabetic retinopathy in various ethnic groups: a worldwide perspective." Survey of Ophthalmology 57.4 (2012): 347-370.
51. Anandhi, S., and K. Anand. "Enhancing Glaucoma Diagnosis with a Novel Optic Disk Localization and Classification Framework Based on U-Net and ResNet-50." 2024 International Conference on Innovative Computing, Intelligent Communication and Smart Electrical Systems (ICSES). IEEE, 2024.

Received: August 15, 2025